Heliyon 8 (2022) e10305

Contents lists available at ScienceDirect

Heliyon

journal homepage: www.cell.com/heliyon

Research article

Thermochemical study of Cr(VI) sequestration onto chemically modified *Areca catechu* and its recovery by desorptive precipitation method

Prabin Basnet [a,c], Pawan Kumar Ojha [a], Deepak Gyawali [a,b], Kedar Nath Ghimire [a], Hari Paudyal [a,*]

[a] Central Department of Chemistry, Tribhuvan University, Kirtipur, Kathmandu, Nepal
[b] Ministry of Forests and Environment, Department of Environment, Government of Nepal, Nepal
[c] Nepal Engineering College, Pokhara University, Changunarayan, Bhaktapur, Nepal

ARTICLE INFO

Keywords:
Betel nut waste
H_2SO_4 charring
Cr(VI) sequestration
Interfering ions
Thermodynamics
$BaCrO_4$ precipitate

ABSTRACT

A new biosorbent for Cr(VI) sequestration was investigated from betel nut waste (BNW), *Areca catechu*, by H_2SO_4 charring. Aqueous insolubility and Cr(VI) uptake capacity of native BNW were potentially improved after H_2SO_4 modification due to cross-linking reaction of betel nut cellulose, thereby creating suitable complexation sites for Cr(VI) ion removal. Langmuir isotherm and pseudo second order (PSO) kinetic models described well with the experimental data. A trace amount of Cr(VI) was effectively removed below the safe drinking water standard (WHO, 0.05 mg/L) using charred BNW (CBNW). The negative value of $\Delta G°$ evaluated for all the temperatures suggested the spontaneous nature of Cr(VI) sequestration and positive value of $\Delta H°$ (42.43±0.13 kJ/mol) confirmed an endothermic reaction. Co-existing NO_3^-, Cl^-, Na^+ and Zn^{2+} ions showed negligible interferences, whereas SO_4^{2-} and PO_4^{3-} notably reduced Cr(VI) uptake capacity of CBNW. More than 98% of adsorbed Cr(VI) was desorbed using 1M NaOH solution. A light yellow precipitate of $BaCrO_4$ was recovered from the desorbed solution after precipitation with $BaCl_2$ solution. Therefore, the CBNW biosorbent investigated in this work is expected to be a promising material for Cr(VI) sequestration and its recovery from polluted water.

1. Introduction

Due to urbanization and industrialization, a large volume of organic pollutants and heavy metal ions have been discharged into the natural environment [1, 2, 3]. Heavy metal pollution in the aquatic environment is now a worldwide concern, posing a serious threat to human health and environmental sustainability due to their strong bioaccumulation, easily penetrating nature, and toxic effect on our bodies [4]. Among the various heavy metals, chromium is one of the most frequently used metal contaminants and is categorized under the top 20 pollutants [5]. Chromium is found in nature in two oxidation states: trivalent and hexavalent, and it can last for a long time. Cr(III) is required for human glucose metabolism in trace amounts, whereas Cr(VI) is toxic and carcinogenic even at low concentrations, causing adverse health effects such as liver disease, kidney damage, internal bleeding, chronic bronchitis, emphysema, skin, lung, and stomach cancer [6, 7, 8]. As a result, the World Health Organization (WHO) sets the highest concentration of Cr(VI) levels as 0.05 mg/L in drinking water [9, 10]. Chromium and its compounds are widely used in several industries such as electroplating, tanning, photography, textile, cement, paints, and metallurgy [11, 12]. Wastewater from those industries produces a large amount of contaminated water containing high concentrations of chromium. Hence, it is necessary to treat that effluent before discharging it into the natural water bodies [12]. Nowadays, various methods such as reduction, suspension, chemical precipitation, ion exchange, solvent extraction, reverse osmosis, membrane separation, electrochemical process, and sorption have been used for Cr(VI) removal from water [13, 14, 15].

Among these, the sorption of heavy metals including chromium using agricultural waste-based biosorbents and biochar looks more promising because of their functional group diversity, ease of modification, high sorption potential, and degradable nature [1, 2, 16]. Various agricultural waste biomasses such as grape waste, groundnut husk, and persimmon waste have been reported to be effective for Cr(VI) remediation from water [17, 18, 19]. Literature shows that the majority of biosorption research for Cr(VI) removal is carried out in batch mode

* Corresponding author.
E-mail address: haripaudyal9@gmail.com (H. Paudyal).

https://doi.org/10.1016/j.heliyon.2022.e10305
Received 12 March 2022; Received in revised form 28 May 2022; Accepted 11 August 2022

[20, 22, 23]; however, removal and recovery of Cr(VI) in continuous systems are rarely done, which are of major concern in the practical use of investigated biosorbent. Therefore, the present research was carried out in both batches as well as column mode for Cr(VI) biosorption using biosorbent prepared from waste biomass of betel nut, *Areca catechu*.

A. catechu is one of the very popular agricultural products and is locally known as Supari in Nepal. Nepal is the third-largest country for *A. catechu* production in the world. A large volume of *A. catechu* waste is produced annually which is usually dumped or sometimes composted for solid waste management. Leaf-sheath of the *A. catechu* is commonly used for the preparation of disposable plates and cups in Nepal whereas the seeds are used for making pan masala, relaxing food ingredients, and dye-fixing agents which are commercial products. However, the solid byproduct obtained after peeling of *A. catechu* seed, some leaf waste, and stem bark are generally dumped in open dumping sites which after decaying in the rainy season produced unpleasant smell and its leachate also polluted the nearby water resources. The fabrication of value-added substance from such waste material for toxic heavy metal removal looks more promising from the viewpoint of improving the economic status of *A. catechu* farmers and environmental remediation. Several studies have been conducted using *A. catechu* biomass for the removal of heavy metals such as Cd(II), Pb(II), Cr(III) without modification [24], Cu(II), Cd(II) by base treatment [25], Fe(II) by pyrolyzed product of betel nut waste [26], and Pb(II) by H_2O_2 modified betel nut waste [27].

In the present investigation, a new adsorbent for effective sequestration of Cr(VI) was developed by charring the waste biomass of *A. catechu* derived after peeling the seed, wasted leaf, and bark with concentrated H_2SO_4. Cr(VI) uptake by modified biosorbent was studied in batch as well as continuous mode. The thermochemical behavior of the investigated biosorbent was also tested together with the desorption, regeneration, biosorbent stability, and its possible reusability in various cycles. The mechanism of Cr(VI) sorption was examined by evaluating the effect of pH, kinetic study, isotherm analysis, dynamic study of a packed column, and characterization techniques such as FTIR, EDX, SEM, and Boehm's titration. More importantly, a new way of desorbing Cr(VI) using alkali solution and its effective recovery as barium chromate precipitate was investigated by desorptive precipitation with barium chloride solution.

2. Materials and method

2.1. Chemicals and analysis

All the chemicals used in this study were of pure analytical grade and were used without further processing. Cr(VI) stock solution (1000 mg/L) was prepared by dissolving 1.415 g of $K_2Cr_2O_7$ in a 500 mL volumetric flask. FTIR spectrophotometer was used to detect several functional groups in the BNW, as well as its alteration after charring and Cr(VI) adsorption (IR Affinity -1S-SHIMADZU spectrometer, Kyoto, Japan). SEM was used to determine the morphological characteristics of the samples (SEM, JEOL model JSM 5900). X-ray diffractograms were acquired by using CuKα ($\lambda = 1.5406$ Å) radiation with 30 mA of current, and 40 kV of voltage in a scan rate of 10°/minutes across the 2θ range of 0 to 80° using an X-ray diffraction spectrometer (Rigaku Co., Japan). EDX spectrometer was used to obtain the energy dispersive X-ray spectra (Shimadzu model, EDX-800HS). The pH of the solution was adjusted by adding a dilute solution of HCl or NaOH (0.1M each) using a pH meter (CHEMI LINE CL-180). The total chromium (Cr) contents in the samples before and after sorption were determined by an atomic absorption spectrometer (Perkin Elmer, USA). The quantities of Cr(VI) existed before and after the Cr(VI) uptake was measured by visual absorbance measurement at 540 nm which was exploited after generating the stable pink color complex when 1,5 diphenyl carbazide was mixed with the Cr(VI) solution in an acidic environment using UV-Vis spectrophotometer (Bio Tek, Synergy LX multimode reader).

2.2. Preparation of biosorbent for Cr(VI) removal

The waste biomass of *A. catechu* (betel nut) was collected from the betel nut farmer of the Jhapa district, located in the Eastern part of Nepal. It was washed several times with double distilled water and dried. Then it was crushed into a fine powder and sieved to particles size of fewer than 150 μm. *A. catechu* peel is rich in cellulose where active sites for Cr(VI) sorption were developed according to the procedure described elsewhere with some modifications as follows [17]. Thirty grams of dried powder of *A. catechu* was mixed with 60 mL of concentrated H_2SO_4 and refluxed for 24 hrs for the charring reaction. Then it was filtered and neutralized using sodium bicarbonate followed by washing several times with double distilled water until neutral pH and dried. The suitable complexation sites for Cr(VI) were developed after the H_2SO_4 treatment where betel nut cellulose underwent a ring-opening reaction according to the mechanism as shown in **supplementary figure 1 (Fig. S1).** The final product obtained in this way is known as charred betel nut waste and abbreviated as CBNW hereafter, which was employed for the Cr(VI) sorption/desorption and recovery test.

2.3. Batch-wise studies

2.3.1. Biosorption of Cr(VI) onto CBNW

Studies of Cr(VI) removal at different pHs were performed by stirring 40 mg of biosorbents (BNW and CBNW each) and 20 mL of Cr(VI) solution (0.19 mmol/L) with a pH variation from 1 to 10. The experiment was also performed with commercial activated carbon and the result was compared with betel nut-based biosorbent for Cr(VI) sequestration. NaOH and HCl solutions were used to adjust the pH values of the Cr(VI) solution. Kinetic studies were performed by varying the contact time at a solid-liquid ratio of 0.5 g/L. Adsorption isotherms were determined by mixing 40 mg of CBNW with 20 mL of Cr(VI) solutions with concentration variations ranging from 0.19 to 9.65 mmol/L at different temperatures. The effect of biosorbent dosage for the removal of Cr(VI) was investigated by varying the amount of CBNW from 0.5 to 8 g/L by using 0.56 mmol/L (29.54 mg/L) of Cr(VI) solution. The samples were shaken for 24 hrs except for kinetic experiments in a mechanical shaker. After stirring at pre-determined intervals of time, the samples were filtered and filtrates were analyzed for Cr(VI) concentration.

$$\%A = \frac{C_i - C_e}{C_i} \times 100 \quad (1)$$

$$q = \frac{C_i - C_e}{W} \times V \quad (2)$$

Where, C_i and C_e are initial and equilibrium Cr(VI) concentrations (mmol/L), respectively. W is the weight of the biosorbent (g) and V is the volume of solution in liter.

2.3.2. Desorption experiment of Cr(VI) from Cr(VI)-CBNW

Prior to the desorption experiment, the Cr(VI) loaded CBNW was prepared as follows. One gram of CBNW was first shacked with 500 mL of Cr(VI) solution (150 mg/L i.e., 2.89 mmol/L) at pH 2 and agitated for 24 hrs to adsorb Cr(VI) onto CBNW. The solid-liquid separation was done by filtration, and the filtrate was tested for residual Cr(VI) content. The residue was washed several times with distilled water to remove unadsorbed Cr(VI) from the CBNW surface and then dried which is known as Cr(VI) loaded CBNW and abbreviated as Cr(VI)-CBNW henceforth. It was used for the desorption experiment. A preliminary experiment for Cr(VI) desorption was carried out using 1M HCl, 1M NaCl, and 1M NaOH solution. NaOH caused the partial dissolution of biosorbent compared to HCl and NaCl. NaOH desorbed 99.72% whereas it was only

12.42% using NaCl solution. From these results, we expect HCl for effective desorption of Cr(VI) ions, however, % desorption is poor (only 34.21%) even using 5M HCl, thus further optimization was carried out using NaOH solution. For this, 50 mg of Cr(VI)-CBNW and 20 mL of NaOH at the varying concentration (0.05 to 2M) were stirred for 6 hrs and then filtered. The percentage desorption of Cr(VI) was determined using the following relationship [28]:

$$\%\ \text{Desorption} = D_{amount}/A_{amount} \times 100 \quad (3)$$

Where A_{amount} (mg/g) is the amount of Cr(VI) adsorbed by CBNW and D_{amount} (mg/g) is the amount of Cr(VI) desorbed from Cr(VI)-CBNW, respectively. To evaluate the stability and reusability of investigated biosorbent, the cycle test of CBNW for Cr(VI) sequestration followed by desorption using NaOH and its re-adsorption test were performed up to five repeated cycles.

2.4. Sequestration of Cr(VI) using fixed bed column packed with CBNW

The dynamic sequestration experiment was carried out in a 20 cm glass column having a 0.8 mm internal diameter. For this, the column was packed with 1 g of CBNW supported with cotton and glass beads. Maximum adsorption of Cr(VI) occurred at pH 2 in batch mode so the column was conditioned by passing water at pH 2 for 12 hrs. Cr(VI) solution (0.082 mmol/L at pH 2) was percolated through the bed of CBNW in the column with a constant flow rate of 16.5 mL/hrs using a peristaltic pump and effluent samples were collected using the fraction collector. The amount of Cr(VI) sorbed onto the bed of CBNW was determined using the following equation [29]:

$$q_{total} = \frac{FA}{1000} = \frac{F}{1000} \times \int_{t_0}^{t_T} C_{ads}\,dt \quad (4)$$

where F is the volumetric flow rate and A is the area under the breakthrough curve.

2.5. Error analysis

To investigate the reproducibility and validation of collected data, error analysis is very important. The experimental data obtained after a triplicate experiment of Cr(VI) adsorption were used to evaluate standard deviations and various other statistical treatments such as regression coefficient (R^2), Chi-square test (χ^2), root-mean-square error (RMSE) and mean absolute error (MAE). The mathematical equations for these expressions are represented as:

$$R^2 = \frac{\sum_{i=1}^{n}(q_{m.e} - q_{m.c})^2 - \sum_{i=1}^{n}(q_{m.e} - q_{m.c})^2}{\sum_{i=1}^{n}(q_{m.e} - q_{m.c})^2} \quad (5)$$

$$\chi^2 = \sum \frac{(q_{m.e} - q_{m.c})^2}{q_{m.c}} \quad (6)$$

$$\text{RMSE} = \sqrt{\left[\frac{\sum_{i=1}^{n}(q_{m.e} - q_{m.c})^2}{n}\right]} \quad (7)$$

$$\text{MAE} = \left(\frac{1}{n}\right)\sum_{i=1}^{n}|q_{m.e} - q_{m.c}| \quad (8)$$

Where, $q_{m.e}$ and $q_{m.c}$ are the experimental and calculated values of the equilibrium biosorption capacities (mg/g), respectively. The lower value of the error function determines the best fit of the mathematical models to the experimental data.

3. Results and discussion

3.1. Characterization of the biosorbents

3.1.1. Chemical modification and crystallinity of the biosorbent

The amorphous structure of the biosorbent is suitable for adsorption reactions. FTIR analysis allows for the observation of various active groups on the biosorbent's surface at 4000-400 cm $^{-1}$. The functional groups that belong to the biopolymer are expected to be modified during chemical reactions [30]. The FTIR also provides details regarding changes/modifications to other active groups that may be involved in the adsorbent's synthesis and Cr(VI) sequestration. **Fig. 1** shows the FTIR spectra of BNW, CBNW, and Cr(VI) loaded CBNW. It was noted that in the case of BNW, there appeared a wide peak at 3326.89 cm^{-1} due to the vibration of hydroxyl groups present in cellulose, hemicellulose, lignin, and pectin available on the biomass surface [31, 32]. The peaks observed at 2913.65, 1710.84, 1591.10, 1243.58, and 1026.61 cm $^{-1}$ are due to the vibrations of C-H, COOH, COO^- (asymmetric), COO, and P = O groups [33].

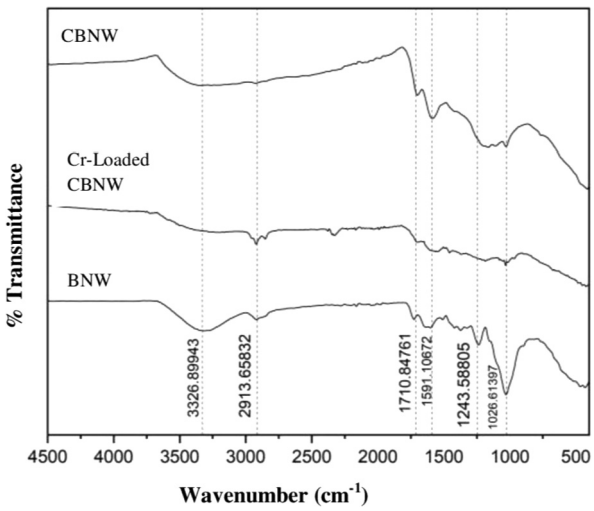

Fig. 1. Analysis of various functional groups in the sample of BNW, CBNW and Cr(VI) loaded CBNW.

However, after charring (CBNW), new peaks corresponding to C–O–C linkages appeared at wave number around 1320 cm^{-1} in addition to the peaks of feed material (BNW), which may be due to the cross-linking condensation reaction of betel nut cellulose with the aid of concentrated sulphuric acid [33]. Moreover, the intensity of the peak due to C=O was increased after sulphuric acid treatment, which may be due to the ring-opening reaction of cellulose as shown in **Supplementary figure 1 (Fig. S1)**.

After Cr(VI) adsorption, the intense peaks observed at wave numbers around 3401, 1624, 1421, 1320, 1086, and 1031 cm^{-1} in CBNW due to the stretching vibration of OH, COO^-(asymmetric), COO^- (symmetric), C–O–C, C–O, and P=O were shifted to 3568, 1645, 1413, 1245, 1097, and 1033 cm^{-1} respectively, suggesting the interaction of these functional groups with Cr(VI) during the adsorption process.

It is well known that the surface of the biosorbent is much more suitable for the adsorption reaction if it is amorphous compared to crystalline. The crystalline property of feed material (BNW) and CBNW were investigated by recording their XRD spectra as shown in **Fig. 2.** It is evident from the results of this figure that BNW possesses the intense peaks corresponding to the crystalline structure of cellulose at 2Θ around 16 and 22 degrees, however in the case of CBNW the crystalline peaks of cellulose at 2Θ around 16 and 22 were disappeared and new band extending from 22.33 to 36.22 degree appeared, suggesting that crystalline nature of betel nut cellulose is converted into amorphous nature after charring reaction. Such an amorphous structure is considered to be more favorable for the adsorption reaction with Cr(VI) ions.

3.1.2. Surface morphology and composition analysis

SEM images of CBNW before and after Cr(VI) adsorption are shown in **Fig. 3(b) and 3(c).** It is observed that the surface of the biosorbent was rough and exhibited ridges or many cracks before Cr(VI) adsorption as shown in **Fig. 3(b).** This can be reasonably attributable

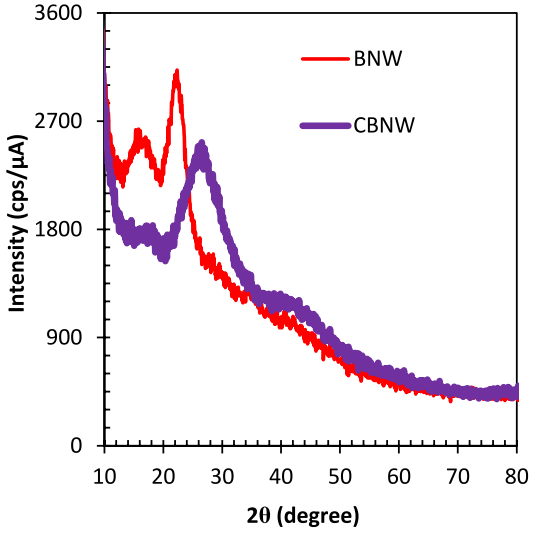

Fig. 2. Powder X-ray diffraction (XRD) patterns of BNW before and after charring at 2θ value from 10 to 80°.

to the structural changes or deformation caused by the charring reaction of BNW cellulose with conc. H_2SO_4. After Cr(VI) adsorption, the surface of the Cr(VI) laden CBNW biosorbent became relatively non-porous and smooth (**Fig. 3(c)**). It strongly indicated that the surface of the CBNW biosorbent was covered by Cr(VI) ion by adsorption reaction which was further evidenced from the EDX spectra of Cr(VI) loaded CBNW as shown in **Fig. 3(a).** Cr(VI) loaded CBNW shows intense peaks corresponding to C, O, and Cr elements at binding energy values of 0.28, 0.51, and 5.41 keV, respectively, suggesting that these were the major elements in Cr(VI) loaded CBNW. Moreover, the observation of 0.97% of chromium in the sample of Cr(VI) loaded CBNW together with 64.75% of carbon and 34.28% of oxygen provides direct evidence that Cr(VI) was effectively sequestered onto investigated CBNW biosorbent.

3.2. Batch-wise studies

3.2.1. Effect of pH and Cr(VI) biosorption mechanism

The pH is a key regulating parameter for the biosorption of Cr(VI) ions because pH changes the Cr(VI) speciation and surface charge of the biosorbent [34]. **Fig. 4** shows the % sequestration of Cr(VI) onto BNW before and after charring and its comparison with the commercially available activated carbon (AC). The result demonstrated a low biosorption percentage of Cr(VI) ions (less than 50% even at optimum pH) onto non-modified BNW whereas it was drastically improved after modification or charring (>97%). The % sequestration of Cr(VI) was maximum at pH 2, and it declined as the equilibrium pH increased for all three biosorbents. The high sequestration % of Cr(VI) onto CBNW also occurred at pH around 2 whereas in the AC it was observed at pH 1. Although the non-modified BNW sequestered around 50% of Cr(VI) at pH 2; however, it was potentially dissolved at acidic conditions (pH = 1 and 2) which was confirmed from the observation of brownish color filtrate after 24 hrs contact with Cr(VI) solution. The dissolution of organic compounds from the CBNW (modified sample) was negligible even in the strongly acidic medium, suggesting that the dissolution of organic compounds from BNW was suppressed by a charring reaction with H_2SO_4. It is considered that some of the low molecular compounds and monomers in BNW were cross-linked together with charring reaction resulting in the improvement of aqueous insolubility. From the speciation diagram, the Cr(VI) mainly exists as hydrogen chromate ($HCrO_4^-$) at pH 0 to 6.5 whereas chromate (CrO_4^{2-}) is dominant at pH higher than 6.5 [21, 30]. However, at the pH below 2, some amount of Cr(VI) ion exists in the form of its neutral species as H_2CrO_4 which was hardly adsorbed onto CBNW reasonably causing the decrease of biosorption percentage of Cr(VI) ions. However, at optimum pH, the Cr(VI) exists in the form of $HCrO_4^-$ anion in water [30, 34], and CBNW also provides suitable moiety for complexation (Scheme 1). With increasing pH (more than 3), the CBNW surface becomes increasingly negative, making the complexation of negatively charged Cr(VI) anions unfavorable, resulting in the reduction of percentage sequestration.

The investigation of the solid phase distribution of adsorbed Cr(VI) onto CBNW is one of the very important parameters for a better understanding of the distribution coefficient for the sequestration process. The distribution coefficient can be determined by using the following relationship:

$$K_D = \frac{C_i - C_e}{C_e} \times \frac{V}{M} \tag{9}$$

Where K_D is the distribution coefficient and M is the mass of the adsorbent used. The relationship between the distribution coefficient of adsorbed Cr(VI) onto the surface of feed material (BNW), CBNW, and commercially available activated carbon (AC) at different pHs is shown in supplementary figure 2 (**Fig. S2**). It shows that the distribution coefficient of Cr(VI) onto activated carbon is maximum at pH 1 whereas it was maximum at pH around 2 in the case of BNW and CBNW. The highest value of K_D observed for BNW, AC and CBNW were evaluated to be 0.61, 50.15, and 147.14 L/g, respectively. This demonstrates that there is an excellent improvement in the uptake of Cr(VI) on the CBNW by the chemical modification.

3.2.2. Effect of contact time or adsorption kinetics

Since native BNW was potentially dissolved in an acidic medium thus application of BNW as a biosorbent for Cr(VI) sequestration was not suitable. So, the effect of other biosorption parameters was investigated only using CBNW. **Fig. 5(a)** depicts CBNW's contact time dependence for Cr(VI) ion sequestration at different pHs. As can be seen from the results, Cr(VI) adsorption onto both biosorbents happens quickly, and the adsorption equilibrium is reached within 45 to 60 minutes. The fast uptake of Cr(VI) may be due to quick exposure of surface active sites of CBNW to Cr(VI) anion, suggesting that surface adsorption of Cr(VI) may be the most likely phenomenon rather than diffusion during the sequestration process. Adsorption kinetics describes the rate of biosorption of Cr(VI) which is one of the most important parameters to design a large industrial-scale operation. To investigate the kinetics of Cr(VI) biosorption, experimental data were analyzed using pseudo-first-order, pseudo-second-order, and intraparticle diffusion models. The exact equation of pseudo-first-order, pseudo-second-order, and intraparticle models can be shown by the equations (equation (10) to (14)) as [35, 36, 37]:

Pseudo-first-order (PFO) model

$$q_t = q_e\left(1 - e^{-k_1 t}\right) \tag{10}$$

$$\log(q_e - q_t) = \log q_e - \frac{k_1}{2.303} t \tag{11}$$

Pseudo-second-order (PSO) model

$$q_t = \frac{k_2 {q_e}^2 t}{1 + k_2 q_e t} \tag{12}$$

$$\frac{t}{q_t} = \frac{1}{k_2 {q_e}^2} + \frac{1}{q_e} t \tag{13}$$

Intra particle diffusion (IPD) model

$$q_t = k_{IPD} \times \sqrt{t} + C \tag{14}$$

Where q_e denotes equilibrium uptake capacity and q_t the uptake capacity at time t. The rate constants for the pseudo-first-order (PFO), intra-particle diffusion (IPD), and pseudo-second-order (PSO) models are represented by k_1, k_{IPD}, and k_2, respectively. These values were evaluated from their respective plots as shown in **Fig. 5(b), Fig. 5(c), and Fig. 5(d)**. The correlation regression coefficient for PFO ranges

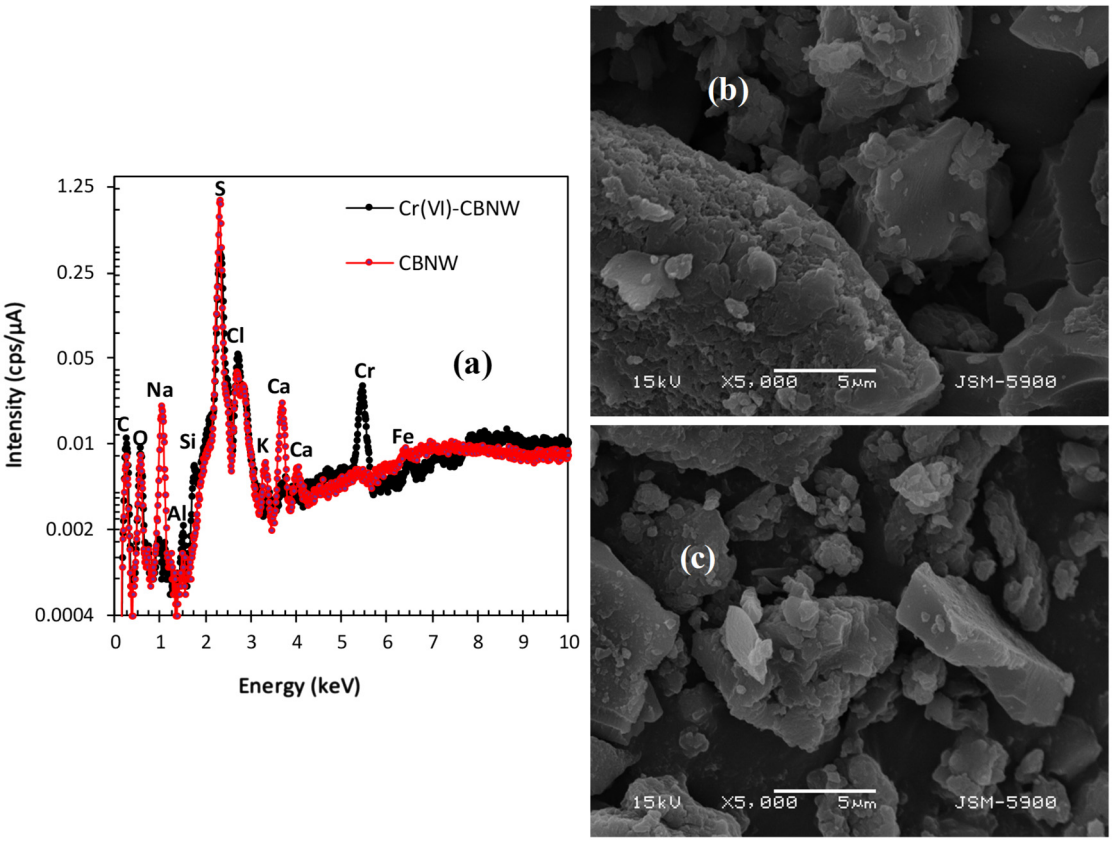

Fig. 3. An elemental analysis and surface morphology of CBNW before and after Cr(VI) sorption (a) EDX spectra, and (b) & (c) SEM images.

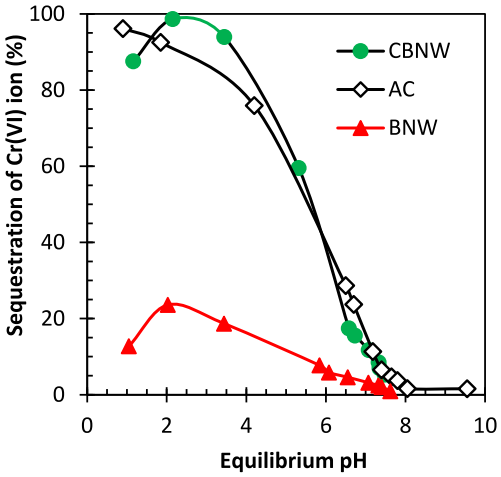

Fig. 4. Sequestration of Cr(VI) using native BNW, CBNW and activated carbon (AC) at different pH. **Condition:** weight of CBNW = 40 mg, volume of solution = 20 mL, Cr(VI) concentration = 0.45 mmol/L, shaking time = 24 hrs, and temperature = 298 ± 2K.

from 0.93 to 0.96 whereas it is between 0.93 and 0.97 for IPD, however, its value is higher than 0.99 in the case of the PSO model for all the tested pHs as shown in **Table 1**. The Cr(VI) uptake capacity determined from the PSO model for all the pHs was found to be much closer to experimental uptake capacity than the PFO and IPD models. Therefore, the rate-limiting step may be chemisorption involving the interaction between the active sites of CBNW and Cr(VI) anion through sharing or transfer of electrons during the sorption process. Moreover, the nonlinear isotherm modeling of experimental data using IPD, PFO, and PSO was done using the experimental data at pH 2 to determine Cr(VI) uptake capacity at a different contact time and evaluated values were plotted together with experimental data in **supplementary figure 3(a)-(d) (Fig. S3)**. The results show that the value of Cr(VI) uptake capacity determined using nonlinear modeling of PSO nearly matches with experimental data which further confirmed the applicability of the PSO model for the description of bio-sorption kinetics of Cr(VI) onto CBNW biosorbent.

3.2.3. *Biosorption isotherm of Cr(VI) ions*

The biosorption isotherm describes the relationship between the amount of adsorbate adsorbed by the biosorbent and its equilibrium concentration. The maximal adsorption capacity of CBNW for Cr(VI) at four different temperatures namely 288, 298, 308 and 318 K were determined using equilibrium adsorption studies, as illustrated in **Fig. 6(a)**. It shows that the Cr(VI) uptake capacity of CBNW was found to increase with the increase of equilibrium concentration of Cr(VI) ion at lower concentrations whereas its values reached the highest value and attained a plateau at a higher concentration for all the temperatures. The Cr(VI) adsorption capacity of CBNW increased with the increase of temperature indicating the characteristics of endothermic reaction which will be further proved by evaluating thermodynamic parameters in section 3.2.4. Freundlich, Temkin, and Langmuir's isotherm equations were used to investigate the best fit model and assess the experimental results [38]. The equations that described the expression of nonlinear and linear forms of the Freundlich isotherm are represented by equations (15) and (16) [38, 39].

$$q_e = K_F C_e^{1/n} \tag{15}$$

$$\log q_e = \log K_F + (1/n) \log C_e \tag{16}$$

Where K_F and n are Freundlich constants that relate to sorption capacity and intensity, respectively. From the intercept and slope of the log q_e vs log C_e plot (**Fig. 6(b)**), the values of K_F (0.84 ± 0.015, 0.99 ± 0.017,

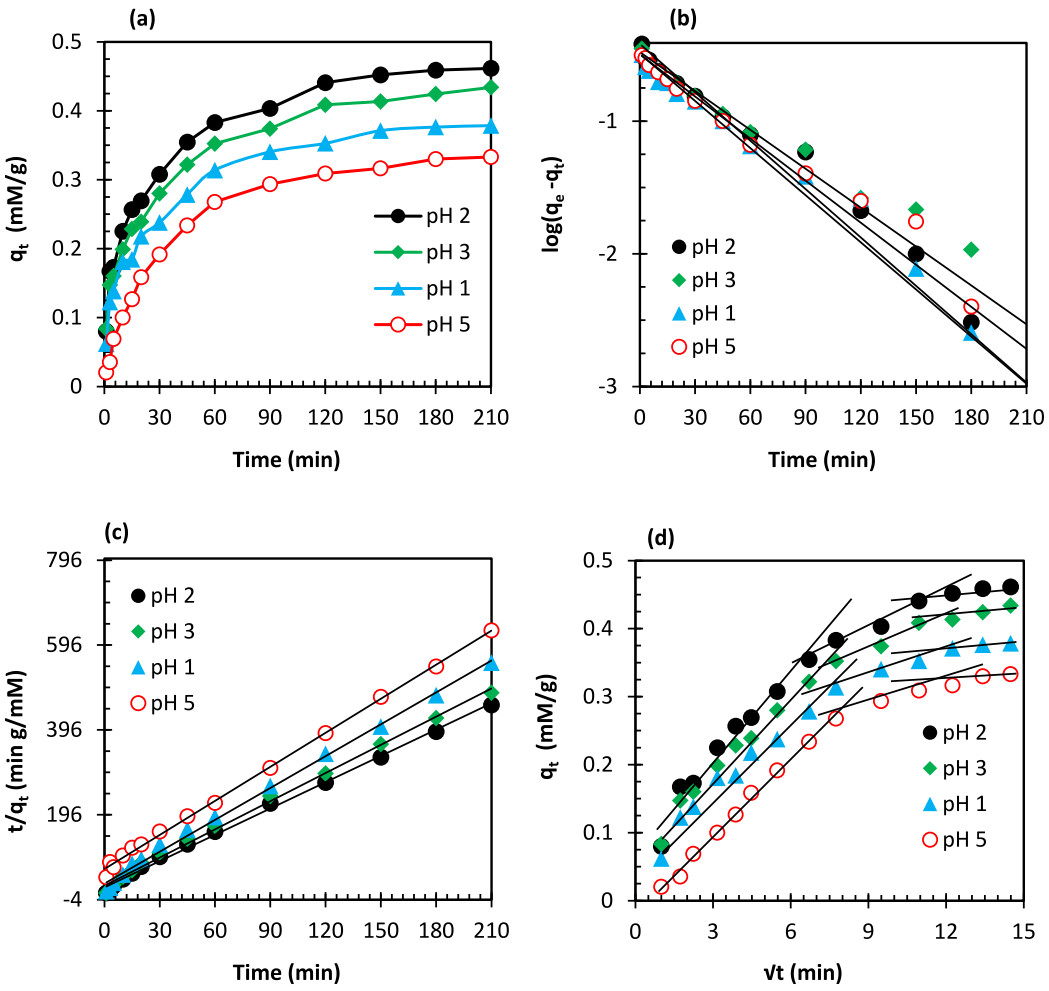

Fig. 5. Biosorption kinetics of Cr(VI) using CBNW at different pH (a) experimental data, (b) pseudo first order (PFO) plots, (c) pseudo second order (PSO) plots, and (d) intra-particle diffusion (IPD) plots. **Condition:** solid liquid ratio = 1 g/L, pH = 2, Cr(VI) ion = 0.45 mmol/L, shaking time = 24 hrs, and temperature = 298 ± 2K.

1.10 ± 0.013 and 1.22 ± 0.015 mmol/g) (L/mmol)$^{1/n}$) and 1/n (0.28 ± 0.02, 0.19 ± 0.05, 0.18 ± 0.01, and 0.16 ± 0.03) were determined at temperatures 288, 298, 308 and 318 K, respectively. The following equations can be used to express the nonlinear and linear forms of the Langmuir isotherm model [38, 40].

$$q_e = \frac{bq_{\max}C_e}{1+bC_e} \tag{17}$$

$$\frac{C_e}{q_e} = \frac{C_e}{q_{\max}} + \frac{1}{bq_{\max}} \tag{18}$$

where q_e is the amount of Cr(VI) sorbed by CBNW at equilibrium, C_e is the residual Cr(VI) concentration, q_{max} is the maximum sorption capacity of CBNW for Cr(VI) and b is the equilibrium constant related to the affinity of the sorption sites for Cr(VI) ions. The maximum sorption capacity (1.23 ± 0.12, 1.51 ± 0.10, 1.81 ± 0.07, and 2.05 ± 0.09 mg/g) and sorption equilibrium constant (1.72 ± 0.06, 2.57 ± 0.02, 5.50 ± 0.05 and 8.59 ± 0.03 L/mmol) were determined from the slope and intercept of the linear plot of C_e/q_e *versus* C_e (**Fig. 6(c)**), respectively.

The Temkin model can be expressed in nonlinear (equation (19)) and linear (equation (20)) form by the relation as [38]:

$$q_e = \frac{RT}{b_T}\ln A_T C_e \tag{19}$$

$$q_e = \frac{RT}{b_T}\ln A_T + \frac{RT}{b_T}\ln C_e \tag{20}$$

Where, A_T and b_T are Temkin constants, R is the universal gas constant and T is the absolute temperature. The values of b_T (J mol^{-1}) and A_T (Lg^{-1}) are determined from the slope and intercept of the straight line obtained from the plot of q_e versus $\ln C_e$ as shown in **Fig. 6(d).** All the evaluated values of Langmuir, Freundlich, and Temkin constants are listed in **Table 2**. The experimental Cr(VI) adsorption capacity is in good agreement with the theoretical value determined using the Langmuir and Temkin isotherm models rather than the Freundlich isotherm, as evidenced by the observation of a higher correlation coefficient for both the isotherms than the Freundlich model. In addition to this, the Cr(VI) uptake capacity of investigated CBNW biosorbent at 298 K was evaluated by using nonlinear equations of Temkin, Langmuir, and Freundlich isotherm models and plotted together with experimental data as shown in supplementary figure 4 (**Fig. S4**). The results also demonstrated the very good fitting of experimentally determined Cr(VI) uptake capacity with the value evaluated from the Langmuir and Temkin isotherm models compared to the Freundlich model.

A comparative study of the maximum adsorption capacity of Cr(VI) by various biosorbents [41, 42, 43, 44, 45, 46, 47, 48, 49, 50, 51, 52, 53, 54] is presented together with CBNW in **Table 3**. It is clear from this table that biosorbents such as ground nut husk and neem bark show low adsorption capacity for Cr(VI) ion whereas chemically modified biosorbents such as caffeic acid functionalized corn starch, magnetite immobilized *Lysinibacillus*, and polypyrrole loaded UFB possess high adsorption capacities. The Cr(VI) uptake capacity of CBNW investigated in this study was higher than other biosorbents except magnetite immobilized *Lysinibacillus* reported in the literature [33, 34, 35, 36, 37, 38, 39, 40, 41, 42, 43, 44]. This strongly suggests that the application of CBNW

Table 1. Kinetics parameters evaluated for the adsorption of Cr(VI) using CBNW at different pH.

Kinetic parameters	pH 1	pH 2	pH 3	pH 5
Pseudo first order (PFO) model				
q_{exp} (mM/g)	0.37 ± 0.06	0.47 ± 0.09	0.43 ± 0.08	0.32 ± 0.05
q_{e1st} (mM/g)	0.61 ± 0.09	0.65 ± 0.11	0.62 ± 0.07	0.60 ± 0.10
k_1 (min^{-1})	0.025 ± 0.007	0.027 ± 0.011	0.020 ± 0.008	0.023 ± 0.013
R^2	0.96	0.93	0.95	0.96
$\chi^2 \times 10^2$	9.44 ± 2.63	4.98± 3.11	5.82 ± 2.08	13.06 ± 3.79
RMSE × 10^2	5.76 ± 0.09	3.24 ± 0.21	3.61 ± 0.13	7.84± 0.15
MAE	0.24 ± 0.06	0.18± 0.04	0.19± 0.08	0.28 ± 0.12
Pseudo second order (PSO) model				
q_{e2nd} (mM/g)	0.44 ± 0.05	0.48 ± 0.09	0.39 ± 0.06	0.37 ± 0.08
K_2 (min^{-1})	0.16 ± 0.004	0.17 ± 0.003	0.18 ± 0.006	0.10 ± 0.005
R^2	0.99	0.99	0.99	0.99
$\chi^2 \times 10^2$	1.23 ± 0.03	0.04 ± 0.005	0.10 ± 0.03	0.51 ± 0.09
RMSE × 10^2	0.55 ± 0.05	0.021 ± 0.002	0.041 ± 0.007	0.19 ± 0.05
MAE	0.07 ± 0.003	0.017 ± 0.005	0.02± 0.003	0.04 ± 0.002
Intra particle diffusion (IPD) model				
q_{e2nd} (mM/g)	0.48 ± 0.12	0.57 ± 0.10	0.54 ± 0.12	0.50 ± 0.13
K_{IPD1} (mM g^{-1} min^{-1})	0.034 ± 0.009	0.041 ± 0.008	0.037 ± 0.005	0.037 ± 0.007
R^2	0.96	0.95	0.97	0.97
K_{IPD2} (mM g^{-1} min^{-1})	0.016± 0.003	0.019± 0.005	0.019± 0.002	0.017± 0.007
R^2	0.92	0.97	0.97	0.94
K_{IPD3} (mM g^{-1} min^{-1})	0.007± 0.002	0.006± 0.001	0.007± 0.003	0.007± 0.002
R^2	0.94	0.95	0.96	0.96
$\chi^2 \times 10^2$	3.27 ± 0.47	2.12 ± 0.33	2.81 ± 029	10.12 ± 0.67
RMSE × 10^2	1.21 ± 0.13	1.01 ± 0.08	1.22 ± 0.12	3.24 ± 0.46
MAE	0.11 ± 0.005	0.010 ± 0.002	0.11± 0.006	0.18 ± 0.08

Table 2. Investigated isotherm parameters for the adsorption of Cr(VI) using CBNW.

Isotherm parameters	288 ± 2 K	298 ± 2 K	308 ± 2 K	318 ± 2 K
Langmuir isotherm				
q_{exp} (mM/g)	1.14 ± 0.08	1.45 ± 0.07	1.76 ± 0.06	2.02 ± 0.07
q_m (mM/g)	1.23 ± 0.12	1.51 ± 0.10	1.81 ± 0.07	2.05 ± 0.09
b (L/mM)	1.72 ± 0.06	2.57 ± 0.02	5.50 ± 0.05	8.59 ± 0.03
R^2	0.99	0.99	0.99	0.99
$\chi^2 \times 10^2$	0.65 ± 0.008	0.10 ± 0.003	0.13 ± 0.002	0.043 ± 0.006
RMSE × 10^2	0.81 ± 0.02	0.16 ± 0.01	0.25 ± 0.05	0.03 ± 0.004
MAE	0.09 ± 0.002	0.04 ± 0.001	0.05 ± 0.002	0.03 ± 0.003
Freundlich isotherm				
K_F (mM/g) $(L/mM)^{1/n}$	0.84 ± 0.015	0.99 ± 0.017	1.10 ± 0.013	1.22 ± 0.015
1/n	0.28 ± 0.02	0.19 ± 0.05	0.18 ± 0.01	0.16 ± 0.03
R^2	0.98	0.97	0.98	0.98
$\chi^2 \times 10^2$	10.71 ± 0.17	21.37 ± 0.24	39.60 ± 0.23	52.45 ± 0.29
RMSE × 10^2	9.00 ± 0.27	21.16 ± 0.19	43.56 ± 0.27	64.00 ± 0.45
MAE	0.3 ± 0.03	0.46 ± 0.07	0.66 ± 0.05	0.81 ± 0.08
Temkin isotherm				
q (mmol/g)	1.10 ± 0.35	1.38 ± 0.23	1.72 ± 0.18	1.95 ± 0.29
b_T (kJ/mole)	16.4 ± 0.38	16.08 ± 0.57	13.47 ± 0.61	12.59 ± 0.24
A_T (L g^{-1})	178.56± 17	1110.96± 29	1495.96± 0.23	3216.95± 19
R^2	0.95	0.95	0.96	0.98
$\chi^2 \times 10^2$	0.14 ± 0.021	0.34 ± 0.054	0.09 ± 0.008	0.24 ± 0.042
RMSE × 10^2	0.16 ± 0.035	0.49 ± 0.018	0.17 ± 0.022	0.49 ± 0.0371
MAE	0.043 ± 0.002	0.072 ± 0.004	0.042 ± 0.003	0.072 ± 0.002

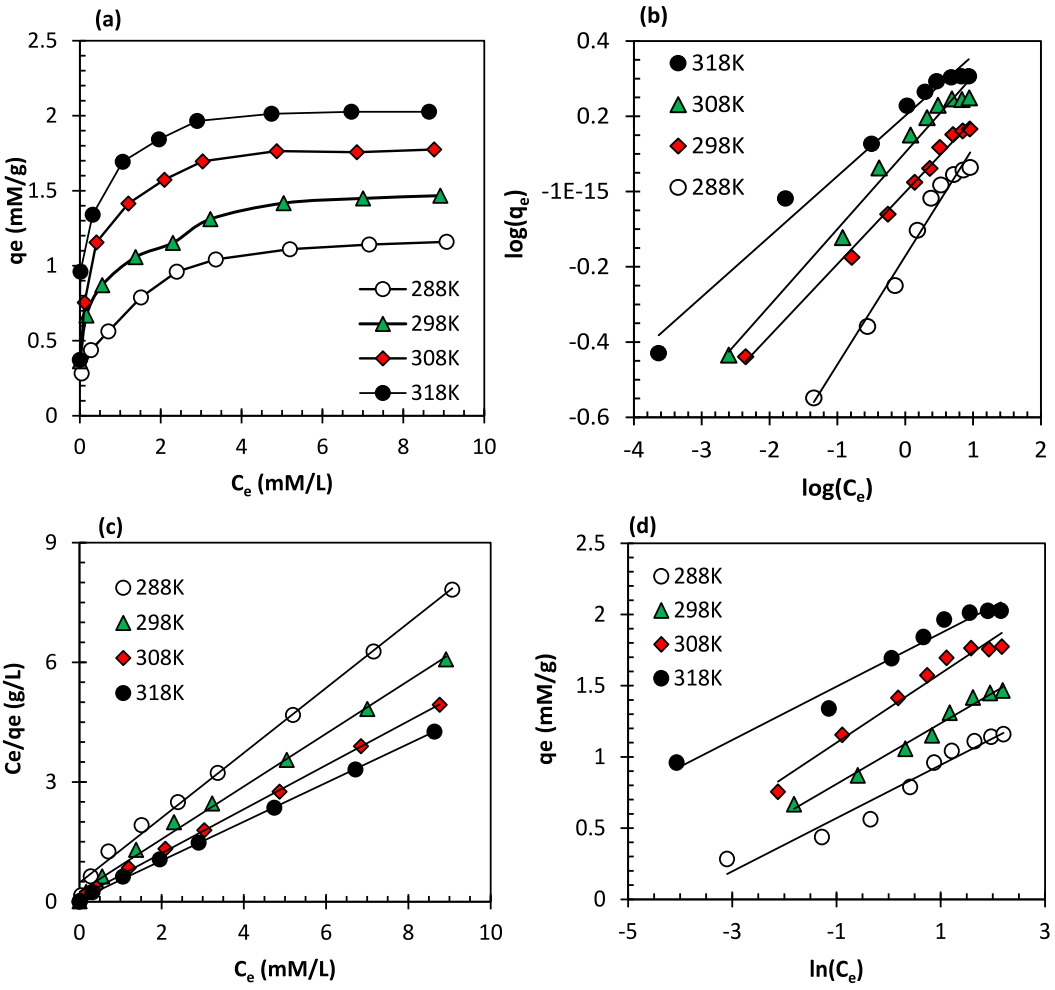

Fig. 6. Biosorption isotherms of Cr(VI) using CBNW at different temperatures (a) experimental data, (b) Freundlich plot, (c) Langmuir plot, and (d) Temkin isotherm model. **Condition:** weight of CBNW = 40 mg, volume of solution = 20 mL, pH =2, and shaking time = 24 hrs.

Table 3. Comparisons of maximum adsorption capacities of CBNW for Cr(VI) investigated in this study with other biosorbents reported in the literature.

Name of biosorbents	pH	S/L ratio (g/L)	Temp. (K)	Maximum adsorption capacity (mmol/g)	References
Biomass-loaded nZVI	3	–	298	1.08	[41]
nZVI-graphene	3	1	*rt	0.47	[42]
Sepiolite-supported nZVI	6	1.6	300	0.84	[43]
Carbon microsphere	4	0.66	298	1.26	[44]
Ground nut husk	3	5	303	0.22	[45]
Coconut fiber	2	2	313	0.42	[46]
Wheat straw	2	1.66	303	1.67	[47]
Barley straw	2	1.66	303	1.68	[47]
Eggshell coated magnetic biosorbent	5.5	8	–	0.74	[48]
Biogas residual slurry	2	4	303	0.11	[49]
Activated rice husk carbon	2	4	–	0.67	[50]
Nanoporous activated neem bark	2.7	6	308	0.52	[51]
Polypyrrole loaded UFB	2	0.5	303	1.67	[52]
Caffic acid functionalized corn starch	3	0.2	333	1.86	[53]
Magnetite immobilized *Lysinibacillus*	9	8	303	2.34	[54]
CBNW	2	2	288	1.23	This work
CBNW	2	2	298	1.51	This work
CBNW	2	2	308	1.81	This work
CBNW	2	2	318	2.05	This work

Note: *rt = room temperature.

Table 4. Estimated thermodynamic parameters for the adsorption of Cr(VI) using CBNW.

Temp. (K)	b (L/mM)	K_C	ΔG^0 (kJ/mol)	ΔH^0 (kJ/mol)	ΔS^0 (J/K mole)
288 ± 2	1.72	95460	−27.45 ± 2.54		
298 ± 2	2.57	142635	−29.40 ± 1.97		
308 ± 2	5.50	305250	−32.34 ± 1.43	42.43 ± 0.13	242.30 ± 5.26
318 ± 2	8.59	476745	−34.56 ± 1.64		

for Cr(VI) removal could be a dual solution for agricultural solid-waste management as well as environmental remediation.

3.2.4. Biosorption thermodynamics

Since sequestration of Cr(VI) was well described using Langmuir type monolayer adsorption model thus thermodynamic parameters were evaluated by using Langmuir equilibrium parameter (b) obtained at different temperatures. The Langmuir equilibrium parameter (b, L/mM) is related to the dimensionless equilibrium constant (K_C) by the relation as [55]:

$$K_C = b(\text{L/mmol}) \times M_{water}(\text{mol/L}) \times 1000 \quad (21)$$

The standard Gibb's free energy change (ΔG°) is related to the equilibrium constant (K_C) by the following expression [56]:

$$\Delta G^\circ = -RT \ln K_C \quad (22)$$

Similarly, the standard Gibb's free energy change of a reaction can be evaluated from the value of standard entropy change (ΔS°) and standard enthalpy change (ΔH°) by using equation (23) [57].

$$\Delta G^\circ = \Delta H^\circ - T\Delta S^\circ \quad (23)$$

From equations (22) and (23) we have

$$\ln(K_C) = -\Delta H^\circ/RT + \Delta S^\circ/R \quad (24)$$

The value of ΔG° for all the tested temperatures was calculated using equation (22) whereas the slope and intercept of Van't Hoff's plot (**Fig. 7**) were used to determine the values of ΔH° and ΔS°, respectively. The evaluated thermodynamic parameters are listed in **Table 4**. The value of ΔG° was found to be negative for all temperatures, implying that Cr(VI) adsorption onto CBNW is spontaneous. Also, the negative value increased with the increase in temperature suggesting that the adsorption is endothermic [58, 59]. The evaluated positive ΔH° value further suggested that the adsorption of Cr(VI) onto CBNW is endothermic. Furthermore, a positive ΔS° indicated an increase in randomness at the interfacial region during Cr(VI) biosorption, which may be owing to the release of some ion/or water molecules during the Cr(VI) sequestration process.

3.2.5. Removal of Cr(VI) from trace concentration

The existence of Cr(VI) in drinking water is harmful even in trace concentrations therefore the ability of investigated CBNW for the removal of trace amount of Cr(VI) from the water was tested. **Fig. 8** shows the comparison of Cr(VI) removal performance of CBNW at pH 1 and pH 2 by varying the biosorbent dose ranging from 0.5 to 8 g/L. The result revealed that the remaining concentration of Cr(VI) was decreased with the increase of CBNW dosage for both the pHs. The remaining concentration of Cr(VI) was reached down to the maximum acceptable limit set by WHO (0.05 mg/L) using only 0.6 g/L of CBNW at pH 2 whereas it required more than 1 g/L to achieve this value at pH 1. From this result, it is concluded that the CBNW investigated in the present work can be a potential material for the treatment of an aqueous solution contaminated with the trace amount of Cr(VI) ions.

3.3. Influence of interfering ions

Cr(VI) pollution in potable water bodies generally occurs naturally due to the weathering of chromium-rich rocks and minerals and anthropogenically by the discharge of wastewater generated from tanning,

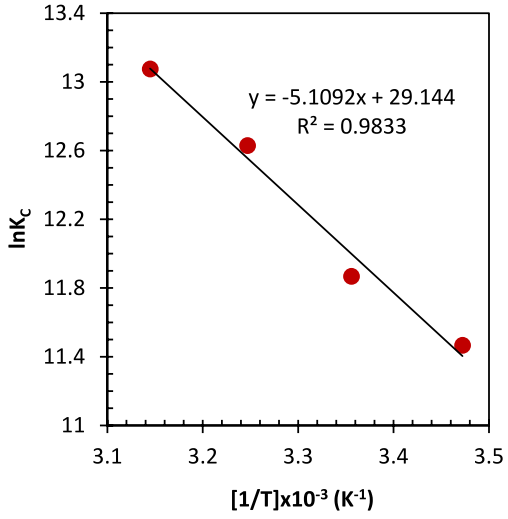

Fig. 7. Van't Hoff's plot for the determination of biosorption thermodynamic during Cr(VI) removal by CBNW.

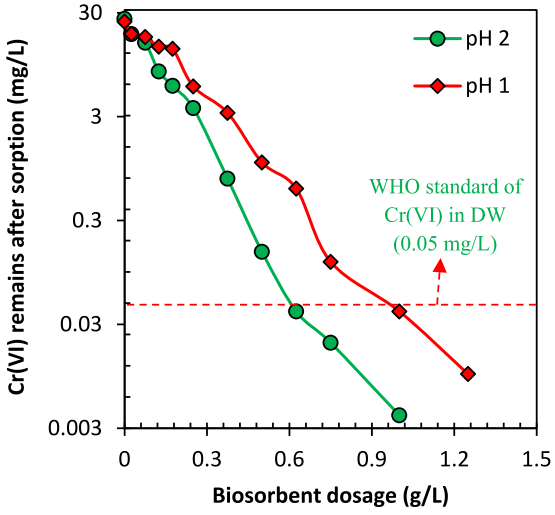

Fig. 8. Influence of CBNW dosage for the removal of Cr(VI) from trace concentration. **Condition:** volume of solution = 10 mL, Cr(VI) concentration = 0.56 mmol/L (29.54 mg/L), shaking time = 24 hrs, and temperature = 298 ± 2K.

paint, electroplating, printing, dyeing, and corrosion inhibitors production. Cr(VI) polluted natural water not only contains chromium ions but also other co-existing ions such as zinc, sulfate, chloride, phosphate, sodium, and nitrate which may potentially interfere with the Cr(VI) adsorption capacity of investigated CBNW biosorbent. **Fig. 9** shows the Cr(VI) uptake capacity of CBNW as a function of varying concentrations of interfering ions. It is evident from the results of this figure that the Cr(VI) uptake capacity of CBNW decreases with the increase of coexisting/interfering ions. Nitrate, chloride, zinc, and sodium have negligible interferences whereas sulfate and phosphate caused the significant lowering of Cr(VI) uptake capacity. The interference effects of tested co-existing ions are in the following order: $PO_4^{3-} > SO_4^{2-} >> NO_3^- \approx Cl^- > Zn \approx Na$. It reveals that the interferences caused by

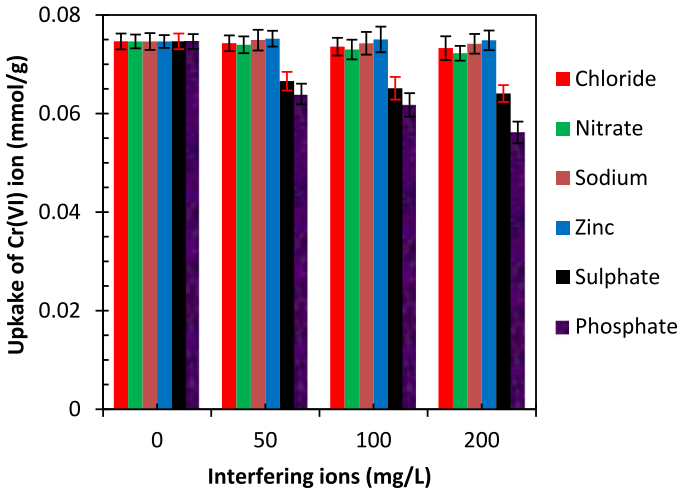

Fig. 9. Effect of interfering ions for the removal of Cr(VI) from water using CBNW. **Condition:** interfering ions = 0 to 200 mg/L, weight of CBNW = 40 mg, volume of solution = 20 mL, pH = 2, Cr(VI) concentration = 0.015 mmol/L, shaking time = 24 hrs, and temperature = 298 ± 2K.

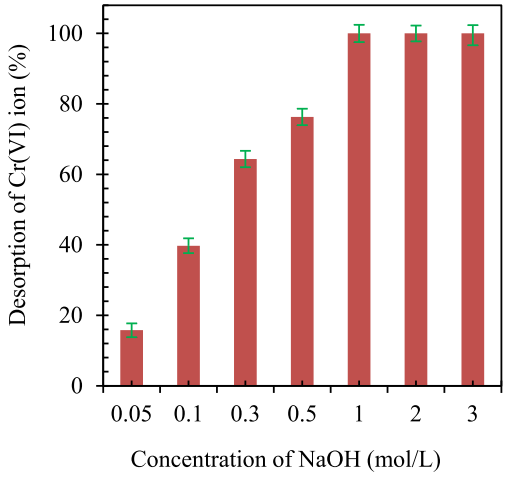

Fig. 10. Regeneration of Cr(VI) loaded CBNW for repeated usage by desorbing Cr(VI) with alkali solution. **Condition:** Cr(VI) content in Cr(VI)-CBNW = 0.04 mmol/g, weight of Cr(VI)-CBNW = 0.05 g, volume of NaOH = 20 mL, shaking = 12 h, and temperature = 298 ± 2K.

cationic species such as zinc and sodium ions are negligible because of their negligible complexation with anionic species of Cr(VI) during the biosorption process. Monovalent nitrate anions caused moderate interferences whereas multivalent anionic species such as sulfate and phosphate possessed significantly high interferences during Cr(VI) sequestration which may be due to the high affinity of these ions with CBNW biosorbent.

3.4. Cr(VI) desorption and its recovery as useful material

3.4.1. Alkaline desorption of Cr(VI) from Cr(VI)-CBNW

It was found from the biosorption test that Cr(VI) biosorption using CBNW is maximum at acidic pH whereas it is insignificant at alkaline medium therefore application of a basic solution for the desorption of spent biosorbent is more effective. Moreover, the maximum desorption of Cr(VI) was observed by NaOH than HCl and NaCl solution from the preliminary experiment. Therefore, in the present investigation, NaOH solution was used as a desorbing agent and its optimization was done by desorbing the Cr(VI) from Cr(VI)-CBNW. **Fig.** 10 depicts the results of a Cr(VI) desorption test with varied concentrations of NaOH solution. It indicates that Cr(VI) desorption increases with increasing NaOH concentration, with 1M NaOH solution achieving over 96% desorption. It is inferred that the chemical bond between the CBNW and Cr(VI) anion is virtually destroyed by alkali solution resulting in the desorption of Cr(VI) anion.

3.4.2. Recovery of desorbed Cr(VI) as useful material

After desorption, a solution containing a high concentration of Cr(VI) is achieved which cannot be directly disposed into the environment because of its toxic and carcinogenic behavior. Thus, recovery of such an aqueous Cr(VI) into solid and useful material is one of the promising options for effective management of desorbed Cr(VI) and production of new Cr(VI) resources. In the present work, the precipitation of chromium solution obtained after desorption is treated with barium chloride ($BaCl_2 \times 2H_2O$) solution to convert it into barium chromate precipitate according to the procedure described elsewhere [60]. The reaction of $BaCl_2$ with the desorbing solution containing a high concentration of Cr(VI) gives a light yellow precipitate of barium chromate ($BaCrO_4$) according to the following equation [60]:

$$Ba^{2+} + CrO_4^{2-} \rightarrow BaCrO_4 \text{ (light yellow ppt)}\downarrow$$

To optimize the precipitation of $BaCrO_4$, the precipitation experiments of desorbed Cr(VI) solution was carried out using 0.3, 0.5, 1, 2, and 3 mmol/L of $BaCl_2$ solutions. The result shows that only 68.34% of Cr(VI) was recovered using 0.3 mmol/L of $BaCl_2$ which was increased to 87.76% at 0.5 mmol/L whereas the recovery reached 98.17% by using 2 mmol/L of $BaCl_2$ solution. The increase in Cr(VI) recovery percentage was insignificant with a further increase in $BaCl_2$ concentration thus 2 mmol/L $BaCl_2$ solutions were optimized for the effective precipitation of desorbed Cr(VI) in the aqueous medium. As a consequence, Cr(VI) ion in the aqueous phase can be recovered into a solid precipitate by this reaction.

For confirmation, the powder XRD patterns of recovered precipitate were compared with the spectrum of pure barium chromate (JCPDS card no. 00-001-1221) as shown in **supplementary figure 5** (**Fig. S5**). It shows that most of the peaks observed in recovered precipitate are exactly in the same position as observed in the case of pure $BaCrO_4$, which provides evidence of the formation of barium chromate precipitate. The recovered $BaCrO_4$ can be used as a Cr(VI) resource for the production of different chromium compounds in addition to its application as an anti-corrosive agent, pigment in paints, ceramics, glasses, porcelains, and also in ignition control devices. Application of such a recovered $BaCrO_4$ derived from the precipitation with $BaCl_2$ in different industries can have greater economic benefit because the market value of $BaCrO_4$ is high as compared to $BaCl_2$ [61].

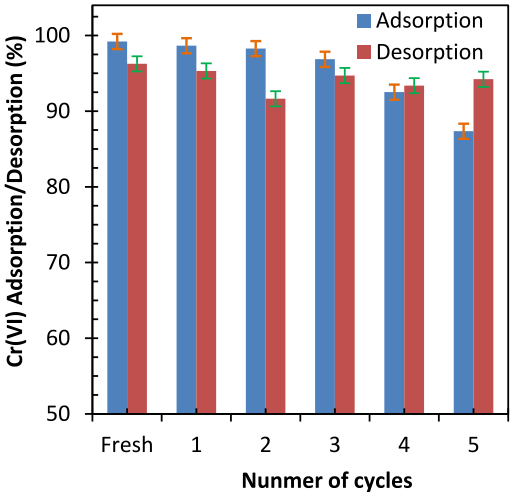

Fig. 11. Cycle test of Cr(VI) biosorption followed by desorption, regeneration and readsorption up to 5 cycles CBNW. **Condition:** Cr(VI) content in Cr(VI)-CBNW = 0.04 mmol/g, weight of Cr(VI)-CBNW = 0.1 g, volume of NaOH = 20 mL, and temperature = 298 ± 2 K.

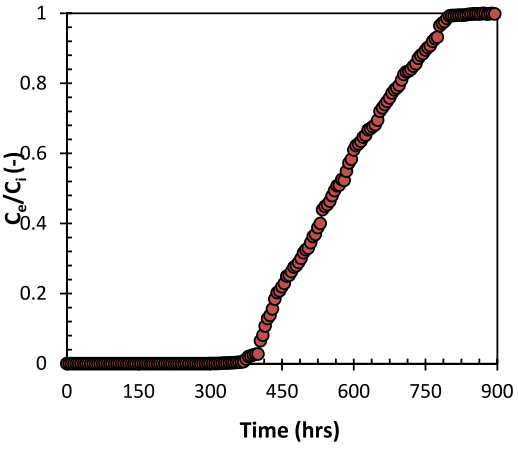

Fig. 12. Dynamic biosorption test of Cr(VI) onto fixed bed column packed with CBNW. **Condition:** Cr(VI) concentration = 0.083 mmol/L, weight of CBNW = 1 g, volumetric flow rate = 16.6 ml/h, pH = 2, and temperature = 298 ± 2 K.

3.5. Biosorbent regeneration and cycle test

NaOH solution was found to be effective for the desorption of Cr(VI) from Cr(VI) loaded CBNW. The surface of the biosorbent is alkaline after desorption using NaOH solution. Thus, it was washed several times with distilled water until getting neutral pH. After that, it was dried and used for re-adsorption experiments in the next cycle. The application of such a spent CBNW for the removal of Cr(VI) in several cycles potentially reduces the water treatment cost. Therefore, the cycle test of Cr(VI) biosorption followed by desorption and re-adsorption was carried out up to 5 repeated cycles as shown in **Fig. 11**. It is evident from the results of this figure that the CBNW removed greater than 97% of Cr(VI) even after 3rd repeated cycle whereas it was observed to be decreased with increasing repeated cycles and reached 87% at the 5th cycle. The reason for decreasing Cr(VI) removal percentage with repeated usage may be due to the leakage of some active sites during biosorbent dissolution. However, the adsorption of Cr(VI) is higher than 87% even after the 5th cycle whereas desorption was higher than 95% in all the cycles. These results show that the CBNW investigated in this study is stable, robust, and has a high potential for adsorptive removal of Cr(VI) from the aqueous solution.

3.6. Cr(VI) sequestration in a packed column system

The break-through profile of Cr(VI) onto the packed column of CBNW is shown in **Fig. 12**. As can be observed from the result of this figure that complete (100%) removal of Cr(VI) can be achieved until 390 hrs then trace concentration of Cr(VI) was detected in the effluents. The saturation of the column occurred after 830 hrs. Maximum Cr(VI) sequestration capacity of investigated CBNW biosorbent in a packed column system was determined to be 0.74 mM/g according to equation (4) (Eq. (4)). The results demonstrate that the Cr(VI) sequestration capacity of CBNW in a dynamic system is less than that observed in batch mode (1.45 mM/g at 308 K) which is due to the possibility of channeling and short contact between biosorbent and Cr(VI) solution [29].

3.7. Mechanism of Cr(VI) biosorption

The results of advanced characterizations and chemical analysis, shifting of various functional groups in FTIR spectra, observation of much smooth surface morphology after adsorption, and detection of chromium in EDX spectrum of Cr(VI) loaded CBNW with a content of 0.97 wt% provide the evidence of effective adsorption of Cr(VI) onto CBNW surface. At lower pH, the surface functional groups in CBNW were protonated to give a positively charged surface where the interaction of negatively charged Cr(VI) species was favored by electrostatic interaction. After the interaction, the adsorption of Cr(VI) anions occurred according to the scheme described in supplementary figure 1 *via* complexation. The observation of suppressed adsorption at higher pHs could be caused by two factors: first, the repulsive force between adsorbate and adsorbent caused Cr(VI) adsorption performance of CBNW, and second, the increased competition between anionic Cr(VI) and hydroxide ions in the bulk decreased the Cr(VI) uptake capacity of investigated biosorbent at higher pH values [53, 62]. In addition to this, due to the existence of reductive functional groups on the CBNW surface, a fraction of Cr(VI) may be reduced to Cr(III) and then bound with carboxyl or hydroxyl groups. Therefore, the biosorbent investigated in this work is expected to provide a significant contribution to the remediation of environmental pollution and the reduction of Cr(VI) toxicity.

4. Conclusion

The cellulose-rich biomass of betel nut waste (BNW) was treated with concentrated H_2SO_4 to achieve CBNW for Cr(VI) sequestration from water. The Cr(VI) removal performance of BNW was greatly increased after H_2SO_4 modification. The removal of Cr(VI) by CBNW is pH-dependent and maximum adsorption occurred at pH 2. The adsorption capacity of CBNW for Cr(VI) was found to increase with increasing temperature. Experimental data were better fitted with Langmuir isotherm and pseudo-second-order (PSO) models. Maximum uptake capacity of CBNW for Cr(VI) was found to be 1.23 ± 0.12, 1.51 ± 0.10, 1.81 ± 0.07 and 2.05 ± 0.09 mmol/g at temperatures 288, 298, 308 and 318 K, respectively, which was better than many biosorbents reported earlier. The value of ΔG^0 for all the temperatures is negative suggesting the spontaneous nature of Cr(VI) adsorption reaction whereas evaluated positive ΔH^0 confirmed endothermic reaction. Cr(VI) was easily desorbed by NaOH solution from Cr(VI) laden CBNW and recovered as $BaCrO_4$ after precipitation with $BaCl_2$ solution. This study provides a new idea to develop an efficient biosorbent for Cr(VI) from betel nut waste together with its novel desorptive precipitative recovery technique, which can be employed for the treatment of Cr(VI) enriched effluents. Therefore it is expected to explore a high-value-added technology for low-cost water treatment as well as an efficient way of recycling waste biomass of betel nut for Cr(VI) treatment.

Declarations

Author contribution statement

Prabin Basnet: Performed the experiments; Analyzed and interpreted the data; Wrote the paper. **Pawan Kumar Ojha:** Performed the preliminary experiments; Wrote the paper. **Kedar Nath Ghimire:** Conceived and designed the experiments; Analyzed and interpreted the data. **Deepak Gyawali:** Analyzed and interpreted the data; Contributed reagents, materials, analysis tools or data. **Hari Paudyal:** Conceived and designed the experiments; Analyzed and interpreted the data; Contributed reagents, materials, analysis tools or data; Wrote the paper.

Funding statement

Pawan Kumar Ojha was supported by University Grants Commission-Nepal [MRS-75/76-S&T-18] for preliminary study.

Data availability statement

Data included in article/supp. material/referenced in article

Declaration of interests statement

The authors declare no conflict of interest.

Additional information

Supplementary content related to this article has been published online at https://doi.org/10.1016/j.heliyon.2022.e10305.

Acknowledgements

The authors are grateful to Dr. Bipeen Dahal, a postdoctoral researcher at Jeonbuk National University in Korea, for scanning electron microscopy (SEM) imaging. FTIR spectra were recorded by Mr. Dipak Kumar Hitan, Department of Customs (Laboratory section), Ministry of Finance, Tripureshwor, Kathmandu, Nepal.

References

[1] M. Qiu, B. Hu, Z. Chen, H. Yang, L. Zhuang, X. Wang, Challenges of organic pollutant photocatalysis by biochar-based catalysts, Biochar 3 (2021) 117–123.
[2] M. Qiu, L. Liu, Q. Ling, Y. Cai, S. Yu, S. Wang, D. Fu, B. Hu, X. Wang, Biochar for the removal of contaminants from soil and water: a review, Biochar 4 (2022) 19.
[3] L. Liang, F. Xi, W. Tan, X. Meng, B. Hu, X. Wang, Review of organic and inorganic pollutants removal by biochar and biochar-based composites, Biochar 3 (2021) 255–281.
[4] S. Shi, J. Yang, M. Li, Q. Gan, K. Xiao, J. Hu, Enhanced Cr(VI) removal from acidic solutions using biochar modified by Fe_3O_4@SiO_2-NH_2 particles, Sci. Total Environ. 628 (2018) 499–508.
[5] T. Jia, B. Zhang, L. Huang, S. Wang, C. Xu, Enhanced sequestration of Cr(VI) by copper doped sulfidated zerovalent iron (SZVI-Cu): characterization, performance, and mechanisms, Chem. Eng. J. 366 (2019) 200–207.
[6] H. Zou, E. Hu, S. Yang, L. Gong, F. He, Chromium(VI) removal by mechanochemically sulfidated zero valent iron and its effect on dechlorination of trichloroethene as a co-contaminant, Sci. Total Environ. 650 (2019) 419–426.
[7] X. Huang, Y. Liu, S. Liu, X. Tan, Y. Ding, G. Zeng, Y. Zhou, M. Zhang, S. Wang, B. Zheng, Effective removal of Cr(VI) using β-cyclodextrin–chitosan modified biochars with adsorption/reduction bifunctional roles, RSC Adv. 6 (1) (2016) 94–104.
[8] J. Zhang, P. Zheng, A preliminary investigation of the mechanism of hexavalent chromium removal by corn-bran residue and derived chars, RSC Adv. 5 (23) (2015) 17768–17774.
[9] P. Veerakumar, P. Thanasekaran, K.C. Lin, S.B. Liu, Biomass derived sheet-like carbon/palladium nanocomposite: an excellent opportunity for reduction of toxic hexavalent chromium, ACS Sustain. Chem. Eng. 5 (6) (2017) 5302–5312.
[10] M.R. Adam, N.M. Salleh, M.H.D. Othman, T. Matsuura, M.H. Ali, M.H. Puteh, A.F. Ismail, M.A. Rahman, J. Jaafar, The adsorptive removal of chromium(VI) in aqueous solution by novel natural zeolite based hollow fiber ceramic membrane, J. Environ. Manag. 224 (2018) 252–262.
[11] E. Malkoc, Y. Nuhoglu, Potential of tea factory waste for chromium(VI) removal from aqueous solutions: thermodynamic and kinetic studies, Sep. Purif. Technol. 54 (3) (2007) 291–298.
[12] C. Xu, W. Yang, W. Liu, H. Sun, C. Jiao, A.J. Lin, Performance and mechanism of Cr(VI) removal by zero-valent iron loaded onto expanded graphite, J. Environ. Sci. 67 (2018) 14–22.
[13] V. Sinha, N.A. Manikandan, K. Pakshirajan, R. Chaturvedi, Continuous removal of Cr(VI) from wastewater by phytoextraction using Tradescantia pallida plant based vertical subsurface flow constructed wetland system, Int. Biodeterior. Biodegrad. 119 (2017) 96–103.
[14] R. Molinari, S. Gallo, P. Argurio, Metal ions removal from wastewater or washing water from contaminated soil by ultrafiltration–complexation, Water Res. 38 (3) (2004) 593–600.
[15] S. Lameiras, C. Quintelas, T. Tavares, Biosorption of Cr(VI) using a bacterial biofilm supported on granular activated carbon and zeolite, Bioresour. Technol. 99 (4) (2008) 801–806.
[16] T. Chen, Z. Zhou, S. Xu, H. Wang, W. Lu, Adsorption behavior comparison of trivalent and hexavalent chromium on biochar derived from municipal sludge, Bioresour. Technol. 190 (2015) 388–394.
[17] K. Inoue, H. Paudyal, H. Nakagawa, H. Kawakita, K. Ohto, Selective adsorption of chromium(VI) from zinc(II) and other metal ions using persimmon waste gel, Hydrometallurgy 104 (2) (2010) 123–128.
[18] U.K. Singh, B. Kumar, Pathways of heavy metals contamination and associated human health risk in Ajay River basin, India, Chemosphere 174 (2017) 183–199.
[19] R. Chand, K. Narimura, H. Kawakita, K. Ohto, T. Watari, K. Inoue, Grape waste as a biosorbent for removing Cr(VI) from aqueous solution, J. Hazard. Mater. 163 (1) (2009) 245–250.
[20] S.P. Dubey, K. Gopal, Adsorption of chromium(VI) on low cost biosorbents derived from agricultural waste material: a comparative study, J. Hazard. Mater. 145 (2007) 465–470.
[21] X. Zhang, S. Zhao, J. Gao, Y. Lei, Y. Yuan, Y. Jiang, Z. Xu, C. He, Microbial action and mechanisms for Cr(VI) removal performance by layered double hydroxide modified zeolite and quartz sand in constructed wetlands, J. Environ. Manag. 246 (2019) 636–646.
[22] Z. Yang, B. Wang, L. Chai, Y. Wang, H. Wang, C. Su, Removal of Cr(III) and Cr(VI) from aqueous solution by adsorption onto sugarcane pulp residue, J. Cent. South Univ. Technol. 16 (2009) 101–107.
[23] R. Li, W. Liang, M. Li, S. Jiang, H. Huang, Z. Zhang, J.J. Wang, M.K. Awasthi, Removal of Cd(II) and Cr(VI) ions by highly cross-linked thiocarbohydrazide-chitosan gel, Int. J. Biol. Macromol. 104 (2017) 1072–1081.
[24] M.A. Rahman, M.A. Hasan, M.A. Salam, A. Salam, N.E.A. Siddique, A.M.S. Alam, Betel-nut Peel as an adsorbent in the removal of Cd, Cr and Pb from aqueous solutions, Pak. J. Anal. Environ. Chem. 13 (2) (2012) 137–147, https://www.researchgate.net/publication/262186883.
[25] W. Zheng, X.M. Li, F. Wang, Q. Yang, P. Deng, G.M. Zeng, Adsorption removal of cadmium and copper from aqueous solution by areca: a food waste, J. Hazard. Mater. 157 (2008) 490–495.
[26] B.S. Subramani, S. Shrihari, B. Manu, K.S. Babunarayan, Evaluation of pyrolyzed areca husk as a potential biosorbent for the removal of Fe(II) ions from aqueous solutions, J. Environ. Manag. 246 (2019) 345–354.
[27] X.M. Li, W. Zheng, D.B. Wang, Q. Yang, J.B. Cao, X. Yue, T.T. Shen, G.M. Zeng, Removal of Pb(II) from aqueous solutions by adsorption onto modified areca waste: kinetic and thermodynamic studies, Desalination 258 (2010) 148–153.
[28] H. Paudyal, K. Inoue, H. Kawakita, K. Ohto, H. Kamata, S. Alam, Recovery of fluoride from water by means of adsorption using orange waste gel followed by desorption using saturated lime water, J. Mater. Cycles Waste Manag. 22 (2020) 1484–1491.
[29] H. Paudyal, B. Pangeni, K. Inoue, H. Kawakita, K. Ohto, S. Alam, Adsorptive removal of fluoride from aqueous medium using a fixed bed column packed with Zr(IV) loaded dried orange juice residue, Bioresour. Technol. 146 (2013) 713–720.
[30] Z. Ren, X. Xu, X. Wang, B. Gao, Q. Yue, W. Song, L. Zhang, H. Wang, FTIR, Raman, and XPS analysis during phosphate, nitrate and Cr(VI) removal by amine cross-linking biosorbent, J. Colloid Interface Sci. 468 (2016) 313–323.
[31] S.L. Goertzen, K.D. Thériault, A.M. Oickle, A.C. Tarasuk, H.A. Andreas, Standardization of the Boehm titration, part I, carbon dioxide expulsion and endpoint determination, Carbon 48 (4) (2010) 1252–1261.
[32] S.S. Ahluwalia, D. Goyal, Microbial and plant derived biomass for removal of heavy metals from wastewater, Bioresour. Technol. 98 (2007) 2243–2257.
[33] B. Pangeni, H. Paudyal, M. Abe, K. Inoue, H. Kawakita, K. Ohto, B.B. Adhikari, S. Alam, Selective recovery of gold using some cross-linked polysaccharide gels, Green Chem. 14 (2012) 1917–1927.
[34] R. Labied, O. Benturki, A.Y. Eddine Hamitouche, A. Donnot, Adsorption of hexavalent chromium by activated carbon obtained from a waste lignocellulosic material (Ziziphus jujuba cores): kinetic, equilibrium, and thermodynamic study, Adsorp. Sci. Technol. 36 (3–4) (2018) 1066–1099.
[35] G. Blanchanchard, M. Maunaye, G. Marti, Removal of heavy metal from water by means of natural zeolites, Water Res. 18 (2) (1984) 1501–1507.
[36] S. Lagergren, Zur theorie der sogenannten adsorption geloester stoffe, Veternskapsakad. Handl. 24 (1898) 1–39.

[37] E.E. Jasper, V.O. Ajibola, J.C. Onwuka, Nonlinear regression analysis of the sorption of crystal violet and methylene blue from aqueous solutions onto an agro-waste derived activated carbon, Appl. Water Sci. 10 (2020) 132.
[38] N. Ayawei, A.N. Ebelegi, D. Wankasi, Modelling and interpretation of adsorption isotherms, J. Chem. 2017 (2017) 3039817.
[39] H. Freundlich, About adsorption in solutions, J. Phys. Chem. 57 (1) (1907) 385–470.
[40] I. Langmuir, The constitution and fundamental properties of solids and liquids, J. Am. Chem. Soc. 38 (1916) 2221–2295.
[41] L. Qian, W. Zhang, J. Yan, L. Han, Y. Chen, D. Ouyang, M. Chen, Nanoscale zero-valent iron supported by biochars produced at different temperatures: synthesis mechanism and effect on Cr(VI) removal, Environ. Pollut. 223 (2017) 153–160.
[42] X. Li, L. Ai, J. Jiang, Nanoscale zerovalent iron decorated on graphene nanosheets for Cr(VI) removal from aqueous solution: surface corrosion retard induced the enhanced performance, Chem. Eng. J. 288 (2016) 789–797.
[43] R. Fu, Y. Yang, Z. Xu, X. Zhang, X. Guo, D. Bi, The removal of chromium(VI) and lead(II) from groundwater using sepiolite-supported nanoscale zero-valent iron (S-NZVI), Chemosphere 138 (2015) 726–734.
[44] J. Han, G. Zhang, L. Zhou, F. Zhan, D. Cai, Z. Wu, Waste carton-derived nanocomposites for efficient removal of hexavalent chromium, Langmuir 34 (21) (2018) 5955–5963.
[45] S.P. Dubey, K. Gopal, Adsorption of chromium(VI) on low cost biosorbents derived from agricultural waste material: a comparative study, J. Hazard. Mater. 145 (2007) 465–470.
[46] D. Mohan, K.P. Singh, V.K. Singh, Removal of hexavalent chromium from aqueous solution using low-cost activated carbons derived from agricultural waste materials and activated carbon fabric cloth, Ind. Eng. Chem. Res. 44 (2005) 1027–1042.
[47] R. Chand, T. Watari, K. Inoue, T. Torikai, M. Yada, Evaluation of wheat straw and barley straw carbon for Cr(VI) adsorption, Sep. Purif. Technol. 65 (2009) 331–336.
[48] T. Ravi, S. Sundararaman, Synthesis and characterization of chicken eggshell powder coated magnetic nano biosorbent by an ultrasonic bath assisted coprecipitation for Cr(VI) removal from its aqueous mixture, J. Environ. Chem. Eng. 8 (2020) 103877.
[49] C. Namasivayam, R.T. Yamuna, Adsorption of chromium(VI) by a low-cost biosorbent: biogas residual slurry, Chemosphere 30 (3) (1995) 561–578.
[50] A. Mullick, S. Moulik, S. Bhattacharjee, Removal of hexavalent chromium from aqueous solutions by low-cost rice husk-based activated carbon: kinetic and thermodynamic studies, Indian Chem. Eng. 60 (1) (2017) 58–71.
[51] U. Maheshwari, S. Gupta, Removal of Cr(VI) from wastewater using a natural nanoporous adsorbent: experimental, kinetic and optimization studies, Adsorp. Sci. Technol. 33 (1) (2015) 71–88.
[52] L. Zhang, W. Niu, J. Sun, Q. Zhou, Efficient removal of Cr(VI) from water by the uniform fiber ball loaded with polypyrrole: static adsorption, dynamic adsorption and mechanism studies, Chemosphere 248 (2020) 126102.
[53] F. Liu, S. Hua, C. Wang, M. Qiu, L. Jin, B. Hu, Adsorption and reduction of Cr(VI) from aqueous solution using cost-effective caffeic acid functionalized corn starch, Chemosphere 279 (2021) 130539.
[54] Y. Zhu, X. He, J. Xu, Z. Fu, S. Wu, J. Ni, B. Hu, Insight into efficient removal of Cr(VI) by magnetite immobilized with Lysinibacillus sp. JLT12: mechanism and performance, Chemosphere 262 (2021) 27901.
[55] X. Zhou, X.I.N. Zhou, The unit problem in the thermodynamic calculation of adsorption using Langmuir equation, Chem. Eng. Commun. 201 (2014) 1459–1467.
[56] H.N. Tran, S.J. You, A.H. Bandegharaei, H.P. Chao, Mistakes and inconsistencies regarding adsorption of contaminants from aqueous solutions: a critical review, Water Res. 120 (2017) 88–116.
[57] F. Xu, H. Chen, Y. Dai, S. Wu, X. Tang, Arsenic adsorption and removal by a new starch stabilized ferromanganese binary oxide in water, J. Environ. Manag. 245 (2019) 160–167.
[58] R.L. Aryal, A. Thapa, B.R. Poudel, B. Dahal, H. Paudyal, K.N. Ghimire, Effective biosorption of arsenic from water using La(III) loaded carboxyl functionalized water melon rind, Arab. J. Chem. 15 (1) (2021) 103674.
[59] B.R. Poudel, R.L. Aryal, S.K. Gautam, K.N. Ghimire, H. Paudyal, M.R. Pokhrel, Effective remediation of arsenate from contaminated water by zirconium modified pomegranate peel as an anion exchanger, J. Environ. Chem. Eng. 9 (2021) 106552.
[60] S. Gupta, B.V. Babu, Removal of toxic metal Cr(VI) from aqueous solutions using sawdust as adsorbent: equilibrium, kinetics and regeneration studies, Chem. Eng. J. 150 (2009) 352–365.
[61] V.I. Mikhaylov, T.P. Maslennikova, E.F. Krivoshapkina, E.M. Tropnikov, P.V. Krivoshapkin, Express Al/Fe oxide–oxyhydroxide sorbent systems for Cr(VI) removal from aqueous solutions, Chem. Eng. J. 350 (2018) 344–355.
[62] R. Liu, Y. Zhang, B. Hu, H. Wang, Improved Pb(II) removal in aqueous solution by ulfide@biochar and polysaccharose-FeS@ biochar composites: efficiencies and mechanisms, Chemosphere 287 (2022) 132087.